Ultrasonic Refractive Index Tomography

C. Pintavirooj†, A. Romputtal†, A. Ngamlamiad†, W. Withayachumnankul‡ and K. Hamamoto*
†Research Center for Communication and Information Technology (ReCCIT), and Department of Electronics, Faculty of Engineering,
‡Department of Information Engineering, Faculty of Engineering,
King Mongkut's Institute of Technology Ladkrabang, Thailand.
*Department of Communications Engineering,
School of Engineering, Tokai University, Japan.
kpchucha@kmitl.ac.th, adisak_romputtal@yahoo.com, s6060510@kmitl.ac.th, kwwithaw@kmitl.ac.th and hama@keyaki.cc.u-tokai.ac.jp

ABSTRACT

Ultrasonic computed tomography (UCT) is one of the methods capable of tissue characterization. It is expected to provide not only a quantitative image but also diagnostic information. As in X-ray CT, UCT requires a projection data to reconstruct a cross-sectional image. In UCT such projection data are derived from the received broadband ultrasonic signal. In this paper, two methods for deriving the integrated refractive index from transmission mode signal are evaluated. The first method derives the integrated refractive index from time delay of the signal while the second method uses the phase shift of signal instead. The experimental results show the resistivity to noise of the phase shift method, especially at the center frequency of the broadband pulse.

Keywords

ultrasound, tomography, refractive index, transmission mode

1. INTRODUCTION

Ultrasound has potentially many important technological applications. These include medical imaging [Jof90], nondestructive testing [Bol89], geophysics [Mol93], and robotic vision [Bol89]. The advantages of microwave and/or ultrasound imaging offered over more conventional imaging are numerous. They include the relatively low health hazard of non-ionizing, low power of sources, such as microwave, ultrasound, etc., its ability to image physiological properties of a tissue or organ, and the likely cost competitiveness of the imaging equipment.

In ultrasound imaging, conventional B-scan image use pulse echo ultrasound reflected from tissue interface to form image as tomography. Pulse-echo B-scan image is not quantitative imaging. Work is now progressing on methods of correlating (quantitatively) these scattered returns with local properties of tissue [Fau83-Kuc94]. This is made difficult by the fact that the scattered returns are modified every time they pass through an interface; hence the interest in computed ultrasonic tomography as an alternative strategy for quantitative imaging with sound. This is mainly due to the fact that ultrasonic computed tomography (UCT) may generate cross-sectional images (tomograms) of three different material properties: (i) an attenuation tomogram representing the ultrasonic energy loss due to scatter and absorption in the material; (ii) a speed-of-sound tomogram representing a measure of the elastic constants in the material [Nie97]; and, (iii) a reflection tomogram representing a map of ultrasonic impedance mismatch from boundaries and inhomogeneities. As a result, ultrasonic computed tomography now receives an intensive attention from many researchers.

Unlike x-ray tomography, the diffraction and refraction of the ultrasonic wave while it gets through the interfaces of the tissue having different reflective indexes make ray travel not in the straight line, hence the line integral geometry as in the X-ray case cannot be implemented here. The approaches to this problem are somewhat complicate, known as the Fourier diffraction theorem [Sla83], the filtered backpropagation algorithm [Dev82] or the algebraic reconstruction algorithm for diffraction tomography [Lad91]. Anyway, one can still use the straight line geometry if assumes the soft tissue has little change

Journal of WSCG, Vol.12, No.1-3, ISSN 1213-6972
WSCG'2004, February 2-6, 2003, Plzen, Czech Republic.

in the refractive indexes. In such case, the traditional filtered back-projection or algebraic reconstruction algorithm for non-diffraction tomography should provide the acceptable results.

UCT can be classified into 2 categories: Ultrasonic Attenuation Tomography and Ultrasonic Refractive Index Tomography. The aim of Ultrasonic Attenuation Tomography is to construct the cross-sectional images of the soft-tissue structures for attenuation coefficient; while the aim of and Ultrasonic Refractive Index Tomography is to make cross-sectional image for refractive index. There exist a number of techniques to measure the projection data. In the class of Ultrasonic Attenuation Tomography, those techniques include Energy-ratio method [Kak78], Division of transforms followed by averaging method [Kak79], Frequency-Shift method [Din79], etc. The projection data of Ultrasonic Refractive Index Tomography mostly based on measurement the time delay [Kak78], which is time difference between ultrasound trasverse with and without object. The time delay is measured between the peak of received ultrasonic pulse collected from both cases. In the presence of noise, however, the time-delay measurement is prone to error due to the presence of noise in the vicinity of peak. This paper purposes the new technique to measure the projection data for of Ultrasonic Refractive Index Tomography which is immune to noise. The measurement is performed in frequency domain by taking FFT of the received ultrasonic pulse. By utilization of time-shifting property of Fourier transform, the projection data is now the phase difference at particular frequency between the FFT of the received Ultrasonic pulse when the ultrasound traverses with no object and FFT of the received Ultrasonic pulse when the ultrasound traverses with object.

The paper is organized as follows. Section 2 presents mathematical models of the transmission mode ultrasonic pulse and the determination of the integrated refractive index from time delay and phase shift. Section 3 shows the acquisition system for gathering the projection from specimen. Section 4 is the experimental results tested on 2 different phantoms showing the reconstructed function of refractive index and sound velocity, including the calculation of error. Section 5 is the discussion and conclusion.

2. REFRACTIVE INDEX TOMOGRAPHY

In ultrasonic tomography, if the change of refractive index along the signal path is gradual, the path can be considered to be direct which means that the effect of diffraction can be omitted. Given the incident signal $x(t)$, one can derive the received signal passing water path $y_w(t)$ in frequency domain regarding to figure 1 by equation 1 [Kak88].

$$Y_w(f) = X(f)H_1(f)H_2(f)\times \exp\left[-\left(\alpha_w(f) + j\beta_w(f)\right)\left(l + l_w\right)\right] \quad (1)$$

where $X(f)$ and $Y_w(f)$ are the Fourier transform of $x(t)$ and $y_w(t)$ respectively, $H_1(f)$ and $H_2(f)$ is the transfer function of the transmitter and receiver, $\alpha_w(f)$ is the frequency-dependent attenuation coefficient of the water, $\beta_w(f)$ is the frequency-dependent phase coefficient of water, l is the thickness of specimen, and $l_w = l_{w1}+l_{w2}$ is the length of water channels.

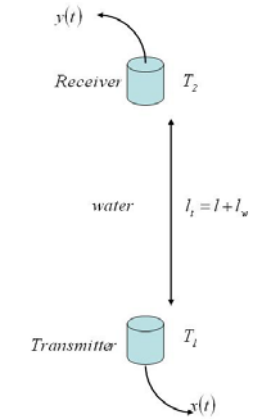

(a)

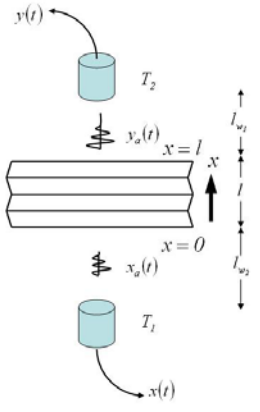

(b)

Figure 1. Ultrasonic signal path (a) without specimen, (b) with specimen.

By passing the signal through the specimen, the received signal $y(t)$ in frequency domain can be written in term of $Y_w(f)$ as following.

$$Y(f) = A_\tau Y_w(f)\exp[-j\beta_w(f)l_w]\times$$
$$\exp\left[-\int_0^l [\alpha(x,f)+j\beta(x,f)]dx\right] \quad (2)$$

Here, A_τ is the attenuation occurring between the junctions of difference refractive index, so-called the transmittance, $\alpha(x,f)$ is the attenuation coefficient at position x, and $\beta(x,f)$ is the phase coefficient at position x. Noted that the attenuation of water is ignored because of the small magnitude compared with the attenuation of specimen. Equation 2 is rearranged to equation 3 and the phase coefficients $\beta(x,f)$ and $\beta_w(f)$ are expressed as $2\pi f/V(x)$ and $2\pi f/V_w$ respectively. $V(x)$ is the propagation velocity of sound at position x and V_w is the propagation velocity of sound in water which is equal to 1483 meters per second.

$$Y(f) = A_\tau Y_w(f)\exp\left[-\int_0^l \alpha(x,f)dx\right]\times$$
$$\exp\left[-j2\pi f\int_0^l\left(\frac{1}{V(x)}-\frac{1}{V_w}\right)dx\right] \quad (3)$$

From equation 3, the signal $Y(f)$ differs from $Y_w(f)$ by two factor, the attenuation and the phase shift. From Fourier transform property, phase shift in frequency domain is equal to time delay in time domain. Therefore, time delay T_d can be expressed as

$$T_d = \int_0^l\left(\frac{1}{V(x)}-\frac{1}{V_w}\right)dx = \frac{1}{V_w}\int_0^l (n(x)-1)dx \quad (4)$$

Using the property of refractive index in equation 5, time delay can be rewritten as equation 6.

$$n(x) = \frac{V_w}{V(x)} \quad (5)$$

$$-V_w T_d = \int_0^l (1-n(x))dx \quad (6)$$

Since time delay is the function of integrated refractive index along the signal path, it can be used as the projection in the reconstruction problem such as filtered-backprojection technique. Practically, time delay of the signal can be measured directly from the delay between peaks of $y(t)$ and $y_w(t)$, or it can be indirectly measured from the phase shift between $Y(f)$ and $Y_w(f)$ as the following.

$$T_d = -\frac{1}{2\pi f}\angle\frac{Y(f)}{Y_w(f)} \quad (7)$$

3. ACQUISITION SYSTEM

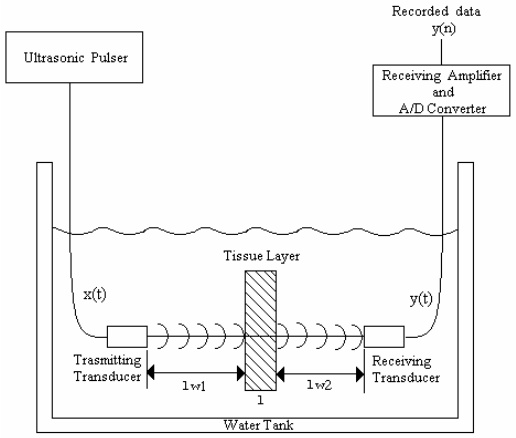

Figure 2. Diagram of the acquisition system

The acquisition system shown in figure 2 consists of

- Specimen's platform capable of moving in the azimuthal direction.
- Water tank used to immerse the specimen. The water helps to couple the signal between the transmitter, the specimen, and the receiver.
- Ultrasonic transmitter and receiver having the center frequency at 3.75MHz. Both are attached to the mechanic arms moving in the horizontal direction.
- Ultrasonic pulse generator which generates the broadband pulse to the transmitter.
- Signal amplifier amplifying the received signal.
- A/D Converter converting the analog signal to digital signal with the sampling rate of 500 MHz.
- Absorber covering the internal wall of tank to prevent the echo of sound.

The diagram of system is shown in figure 2 and the prototype is shown in figure 3.

In order to keep the projection data, the specimen is rotated to the specified angle and then the ultrasonic transmitter and receiver are moved to the 1st projection position. The pulse generator generates ultrasonic broadband pulse to the transmitter, and then the receiver receives the distorted pulse. The pulse is transformed to the digital format by the A/D converter and stored in the computer. When the transmitter and receiver move to the next projection position, the same process starts again. After complete one projection, the specimen is rotated to the new angle and all the processes restarts. In the experiment, the interval of angle is set to 10 degrees, and the interval or resolution between each scanning point is 1 millimeter. Figure 4 shows two types of pulses; the first of which is the reference pulse or $y_w(t)$ collected from sending the pulse through the water and the second is the distorted pulse or $y(t)$ collected from sending the pulse through the specimen.

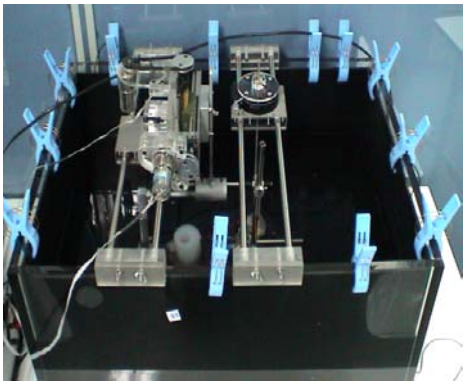

(a)

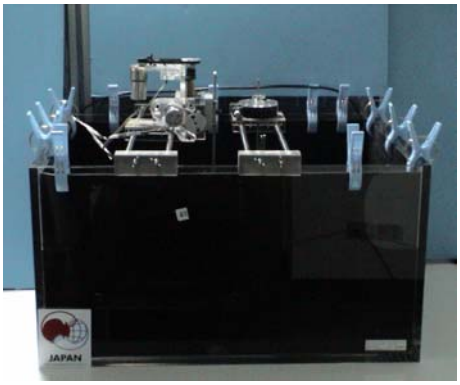

(b)

Figure 3. The prototype of ultrasonic acquisition system (a) top view, (b) side view.

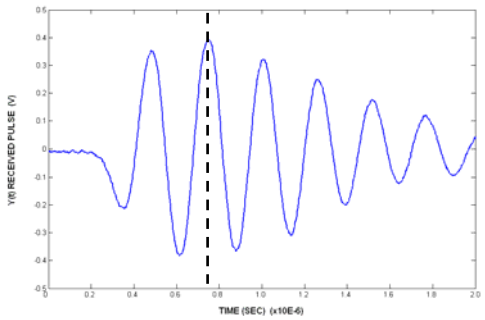

(a)

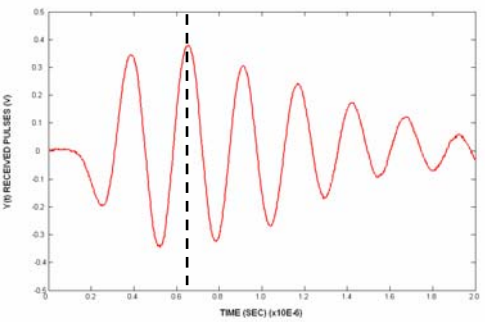

(b)

Figure 4. Two types of pulses, (a) the reference pulse $y_w(t)$ and (b) the distorted pulse $y(t)$.

4. Experimental Results

Two phantoms with different patterns remarked as "A" and "B" are used to evaluate the reconstruction process. The phantoms are made from the gelatin having the refractive index close to the water, and the diameter of each phantom is approximately 60 millimeters.

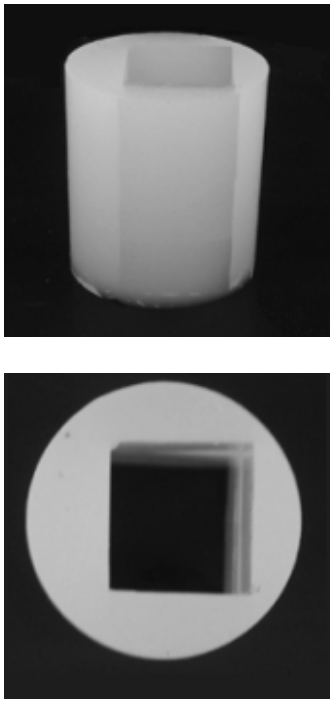

Figure 5. Phantom A, side view and top view.

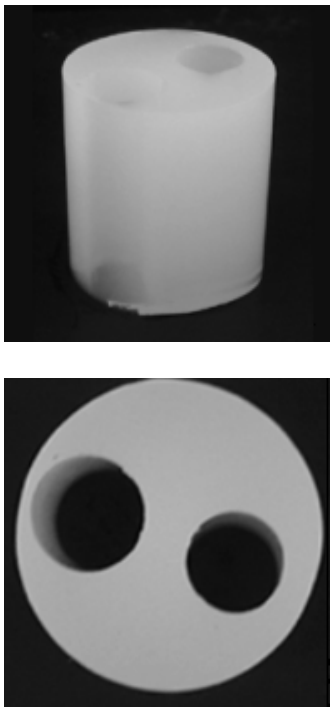

Figure 6. Phantom B, side view and top view.

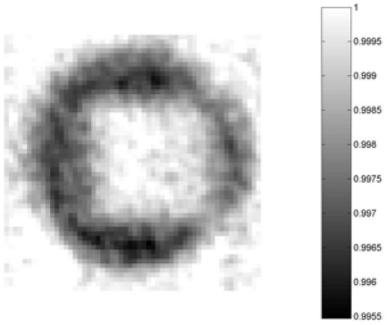

(a)

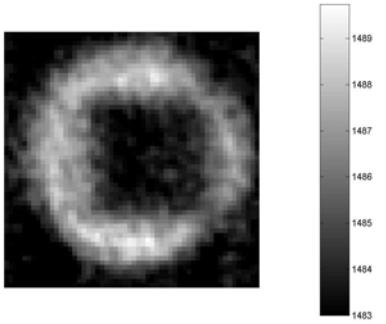

(b)

Figure 7. Reconstruction of (a) refractive index and (b) sound velocity of phantom "A" using time delay.

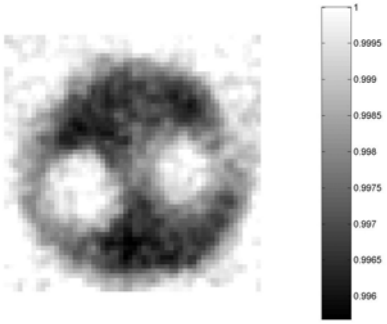

(a)

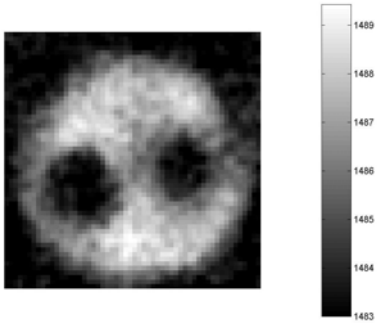

(b)

Figure 8. Reconstruction of (a) refractive index and (b) sound velocity of phantom "B" using time delay.

Two methods are used to solve for the integrated refractive index, the time delay and the phase shift. In the time delay method, T_d is detected from the maximum peak of the broadband pulses whereas in phase shift method, T_d is calculated from equation 7 after taking Fourier transform of the reference and distorted signals. When the set of projections is found, the filtered backprojection with the Hann filter is employed to find the cross-sectional function. By using equation 6 and equation 5, the reconstructed function of refractive index and the reconstructed function of sound velocity can be obtained respectively. The results from time delay are shown in figure 7 and 8, and the results from phase shift at selected frequencies are shown in figure 9 and 10. Table 1 and 2 are correspond to the Mean Square Error of phantom A and B respectively. The formula of MSE is given by

$$MSE = \frac{\iint \left[o(x,y) - o'(x,y) \right]^2 dxdy}{\iint \left[o(x,y) \right]^2 dxdy} \times 100 \qquad (8)$$

where *o(x,y)* denotes the value of the original function, *o'(x,y)* denotes the value of the reconstructed function, both of which are normalized to 0-255. The MSE of both phantoms at different frequencies are also presented in the graphs.

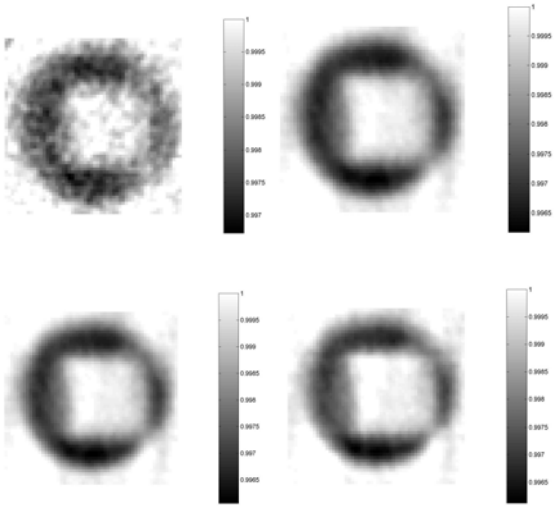

Figure 9. Reconstruction of the refractive index of phantom "A" using phase shift at frequency of 1.5 MHz, 3.5 MHz, 3.75 MHz, and 6MHz respectively.

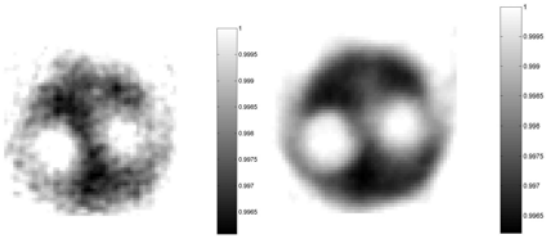

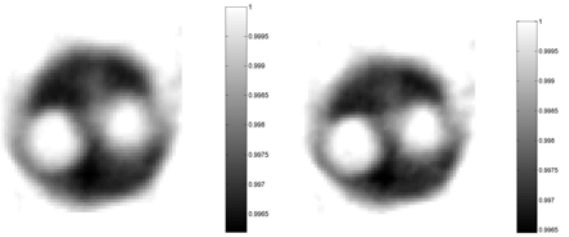

Figure 10. Reconstruction of the refractive index of phantom "B" using phase shift at frequency of 1.5 MHz, 3.5 MHz, 3.75 MHz, and 6 MHz respectively.

Method		Mean Square Error (%)
Time Delay		29.405
Phase Shift at Frequency (MHz)	1.50	30.072
	2.00	26.679
	3.00	25.335
	3.50	25.130
	3.70	25.447
	3.75	**25.308**
	4.00	25.794
	4.25	26.275
	6.00	29.061

Table 1. Mean Square Error of Phantom "A"

Method		Mean Square Error (%)
Time Delay		24.217
Phase Shift at Frequency (MHz)	1.50	28.737
	2.00	23.774
	3.00	22.022
	3.50	22.318
	3.70	21.759
	3.75	**21.259**
	4.00	21.428
	4.25	21.449
	6.00	23.192

Table 2. Mean Square Error of Phantom "B"

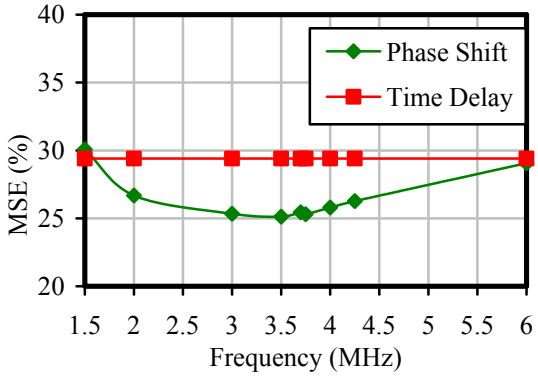

Figure 11. Plotting of the MSE of phantom "A"

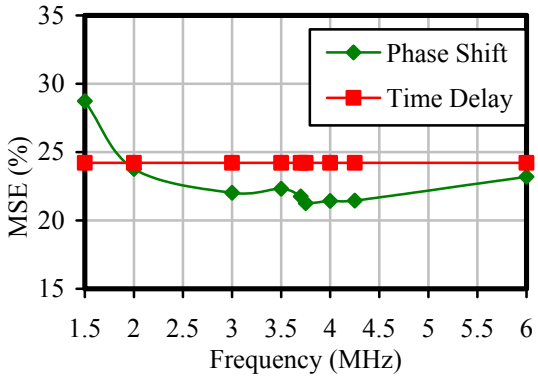

Figure 12. Plotting of the MSE of phantom "B"

5. DISCUSSION AND CONCLUSION

The results from both phantoms show the agreement in every aspect. The reconstructed function obtained from time delay method is so sensitive to noise that it gives the poor quality image. This problem is eliminated in the phase shift method. At the frequency of 3.75 MHz which is the center frequency of the system, the error is lowest compared with its neighbor frequencies. The reconstructed function derived from the center frequency is almost noise-free and therefore the exact value of function can be correctly read out at every point.

In order to find the function of refractive index from broadband ultrasonic pulses, determining the integrated refractive index from phase shift of the signals gives the best results. One can easily select the most suitable frequency which is normally located on the center frequency of the system. Once the function of refractive index is found, it can be turned to the function of sound velocity by the simple relation.

6. ACKNOWLEDGEMENT

The authors would like to thank P. Ungpinitpong, former member of the Biomedical' Laboratory, KMITL and S. Ngamanekrat, member of the Biomedical Laboratory. The researching fund has been kindly supported by JICA.

7. REFERENCES

[Bol89] Bolomey, J., -C., "Recent Eurepean Developments in Active Microwave Imaging for Industrial, Scientific, and Medical Application," *IEEE. Trans. Microwave Theory Tech*., vol. 37., no. 12, pp. 2109-2117, 1989.

[Dev82] A. J. Devaney, "A Filtered Backpropagation Algorithm for Diffraction Tomography" *Ultrason. Imaging*; 1982; 4; p 336-350.

[Din79] Dines, K. A., and Kak, A. C., "Ultrasonic attenuation tomography of soft biological tissues," *Ultrason. Imaging*, vol. 1, pp. 16-33, 1979.

[Fau83] Faux, S. W., Pele, N. J., Glover, G. H., Gutmann, F.D., and Mclachlan, M., "Spectral Characteristics and Attenuation Measurements in Ultrasound," *Ultrason. Imaging*, vol. 5, pp. 95-116, 1983.

[Jof90] Jofre, L., Hasley, M. S., Broquetas, A., Reyes, E., Ferrando, and M. Elias-fuste, "Medical Imagingwith Microwave tomographic Scanner," *IEEE. Trans. Biomed. Eng.,* vol.37, no. 3, pp. 303-312, 1990.

[Kak78] Kak, A. C. and Dine, K. A., "Signal processing of broadband pulsed ultrasound: Measurement of Attenuation of Soft biological tissues" *IEEE Trans. Biomed. Eng.*, vol. BME-25, pp. 321-344, July 1978.

[Kak79] Kak, A. C., " Computerized Tomography with x-ray emission and utrasound sources", *Proc. IEEE,* vol. 67, pp. 1245-1272, 1979.

[Kak88] A. C. Kak, and M. Slaney, "*Princicles of Computerized Tomographic Imaging*", IEEE Press, NY, 1988.

[Kuc94] Kuc, R., "Estimating Acoustic Attenuation from Reflected Ultrasound Signals: Comparison of Spectral- Shift and Spectral-Difference Approaches," *IEEE Trans. Acoust. Speech Signal Processing*, vol. ASSP-32, pp. 1-7, 1994.

[Lad91] K.T. Ladas, A. J. Devaney, "Generalized ART Algorithm for Diffraction Tomography" *Inv. Prob.*; 1991; 7; p 109.

[Mol93] Molyneux, J. E. and Witten, A, "Diffraction Tomographic Imaging in a Monostatic Measurement Environment," *IEEE. Trans. Geosci. Remote Sensing*, vol. 31, no. 2, pp. 507-511, 1993.

[Nie97] Nielsen, S.A. and Andersen, S.I.: 18th *Riso Intern. Symp. on Materials Science*, 1997,1:455-464

[Sla83] M. Slaney, A. C. Kak, "Diffraction Tomography" *Proc. S.P.I.E.*; Apr. 1983; 413; p 2-19.